tive slopes observed for $P(\rho)$ near $\rho = 0$ in Figs. 1(b) and 2(b) imply that the radial coupling assumed by Betz *et al.*[3] cannot be the only source of excitation, since for this mechanism the slope of $P(\rho)$ is expected to be zero for $\rho = 0$.[3] In fact, these $P(\rho)$ distributions suggest that a rotational-coupling mechanism may be involved also. It is of considerable interest to explore these questions in detail. We have demonstrated that the Doppler-shift technique introduced in these experiments provides such an opportunity.

We thank Professor W. Greiner, Professor B. Müller, and Dr. G. Soff for many valuable discussions, and Dr. R. Simon and Dr. H. T. Wollersheim for their assistance. One of the authors (J.S.G.), wants to express his gratitude to the GSI laboratory for the hospitality extended to him, and to the Alexander von Humboldt–Stiftung for support under a Senior U. S. Scientist Award.

[1]H. Backe, E. Berdermann, H. Bokemeyer, J. S. Greenberg, E. Kankeleit, P. Kienle, Ch. Kozhuharov, L. Handschug, Y. Nakayama, L. Richter, H. Stettmier, F. Weik, and R. Willwater, in *Proceedings of the Tenth International Conference on the Physics of Electronic and Atomic Collisions, Paris, 1977* (Commissariat à L'Energie Atomique, Paris), p. 162.

[2]K. Smith, H. Peitz, B. Müller, and W. Greiner, Phys. Rev. Lett. 32, 554 (1974).

[3]W. Betz, G. Soff, B. Müller, and W. Greiner, Phys. Rev. Lett. 37, 1046 (1976).

[4]C. Foster, T. R. Hoogkammer, P. Woerlee, and F. W. Saris, J. Phys. B 9, 1943 (1976).

[5]W. E. Meyerhof, Phys. Rev. A 10, 1005 (1974).

[6]D. Schwalm, A. Bamberger, P. G. Bizzeti, B. Povh, G. A. P. Engelbertnik, J. W. Olness, and E. K. Warburton, Nucl. Phys. A192, 449 (1972).

[7]J. S. Greenberg, H. Bokemeyer, H. Emling, E. Grosse, D. Schwalm, and H. J. Wollersheim, in *Proceedings of the Tenth International Conference on the Physics of Electronic and Atomic Collisions, Paris, 1977* (Commissariat à L'Energie Atomique, Paris), p. 160.

[8]R. Anholt, to be published.

[9]H. H. Behncke, P. Armbruster, F. Folkmann, S. Hagmann, and P. H. Mokler, in *Proceedings of the Tenth International Conference on the Physics of Electronic and Atomic Collisions, Paris, 1977* (Commissariat à L'Energie Atomique, Paris), p. 158.

[10]W. E. Meyerhof, Phys. Rev. Lett. 31, 1341 (1973).

[11]H. H. Behncke, P. Armbruster, F. Folkmann, S. Hagmann, and P. H. Mokler, in *Proceedings of the Tenth International Conference on the Physics of Electronic and Atomic Collisions, Paris, 1977* (Commissariat à L'Energie Atomique, Paris), p. 156.

Particle-Caviton Interactions

A. Y. Wong, P. Leung, and D. Eggleston
Department of Physics, University of California, Los Angeles, California 90024
(Received 10 August 1977)

Experiments using a controlled electron beam interacting with a caviton containing coherent rf fields demonstrate the importance of transit-time damping of localized high-frequency fields. A small transverse magnetic field ($B \leq 10$ G, $\omega_c/\omega_p \leq 0.1$) was sufficient to eliminate such transit-time damping. A modulated electron beam is used to demonstrate that the interaction between the beam and the caviton field is phase sensitive. Regeneration of cavitons by streaming particles is discussed.

We wish to report experiments which demonstrate that localized oscillating fields together with their density perturbations (hereafter referred to as cavitons[1]) are sensitively dependent on the ambient background electron distribution function. Our experiments consist of monitoring the amplitude of the localized electric field of the caviton in the presence of an electron distribution whose fast-electron population can be controlled. Our results agree with recent theoretical studies[2-4] on the effective energy exchange between cavitons and particles and the role of this interaction in determining the saturation value of localized fields.

Our first experiment is performed in a modified double-plasma device.[1,5] A density gradient is formed in the target side by arranging the filaments preferentially. Our operation conditions are $kT_e \approx 2$ eV, $T_e/T_i \approx 10$, $n \approx 10^9$ cm^{-3}, $n_0/\nabla n_0 \approx 25$ cm, and $\gamma_{en}/\omega_p \approx 10^{-3}$. A quasistatic external rf field ($\omega_0/2\pi \approx 300$ MHz) is imposed on the plasma by applying a signal to an antenna located at the low-density side of the chamber ($\xi_0 \approx 3$ V/cm). At the resonance region an intense local-

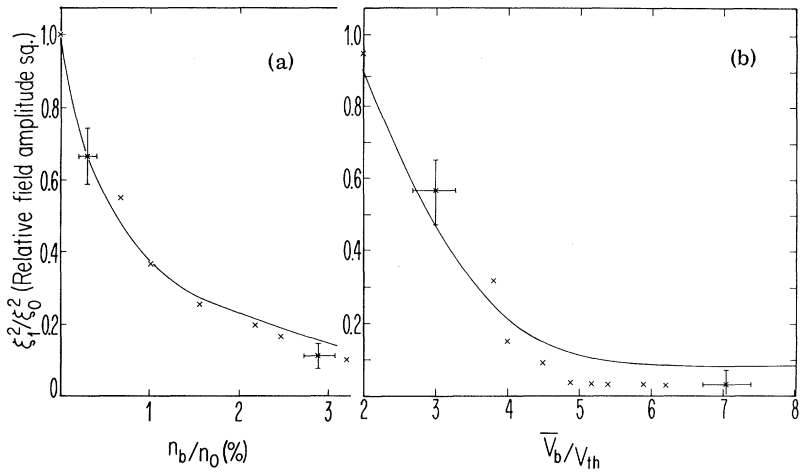

FIG. 1. (a) Relative electric field intensity vs the density of the electron beam at $\bar{v}_b/\bar{v}_{th}=4.5$. ξ_1 is the electric field in the presence of the beam, ξ_0 the electric field without the injected beam. The solid curve is obtained by using Eq. (2) where the wave convection loss term is obtained from one experimental point. This gives a value of $V_g \approx 0.008V_{th}$, which agrees with the value of V_g measured [(0.007 to 0.01)V_{th}] in previous caviton experiments (Ref. 7). (b) The relative electric field intensity vs the velocity of the electron beam for $n_b/n_0 \approx 2.5\%$. The solid curve is Eq. (2).

ized electric field and a density perturbation or caviton are produced ($\xi^2/4\pi n_0 T \approx 1$). The caviton is essentially one dimensional with an axial width of $20\lambda_D$ and a transverse dimension of $600\lambda_D$. The magnitude of the electric field is measured by a diagnostic electron gun[1,6] (5–9 keV, 100 nA, $n_b \approx 10^4$ cm^{-3}) in the radial direction. A controlled electron beam of variable energy ($\frac{1}{2}mv_b^2 \leq 150$ eV, $\Delta v_b/v_b \approx \frac{1}{3}$) and density ($n_b/n_0 \approx 0.5\%$ to 4%) can be launched from the source side into the target side along the axial direction by suitably biasing the two separation grids. The resulting electron distribution is measured with a disk probe, whose current-voltage characteristic is differentiated by an on-line computer. The beam density is obtained by integration of the beam distribution.

Under our operating conditions the effect of collisional damping on the electric field is negligible and the density gradient remains unchanged under the injection of our controlled electron beam. The sensitive dependence of the electric field intensity ξ^2 inside the caviton on the beam density n_b at a fixed beam velocity is shown in Fig. 1(a). With a beam density as low as $n_b/n_0 \approx 0.6\%$, ξ^2 is reduced to half the intensity obtained without the injected beam. The interaction also reveals the preferential scattering of electrons at high velocities as shown in Fig. 1(b). When $\bar{v}_b \approx 3v_{th}$, the field intensity drops to half its initial value. For a caviton width of $20\lambda_D$, particles with $v > 3v_{th}$ make a transit through the characteristic width of the caviton in around one period.

One method to reduce transit-time damping is to impose a transverse magnetic field such that particles cannot freely stream through the caviton regions. In our second experiment[8] a weak and uniform magnetic field ($\omega_c/\omega_p \leq 0.1$) is produced by two large Helmholtz coils (50 cm in diameter). In a steady-state discharge plasma the electron distribution consists of background plasma with temperature $T_e \approx 2$ eV and a small percentage of primary electrons ($n_p/n_0 \approx 0.5\%$) with energy 30–40 eV. Both types of electrons can contribute to transit-time damping, but the primary electrons make a larger contribution because they can traverse the caviton in less than one period. When a magnetic field is turned on ($B \approx 2$ G), most of the background electrons are restricted to small circular orbits with $r \leq 20\lambda_D$ and are rendered ineffective in causing transit-time damping. The caviton field therefore starts to increase with the imposed magnetic field (see Fig. 2). At a larger magnetic field ($B = 7$ G), where the fast electrons have gyroradii comparable to the distance between discharge filaments and caviton, the population of fast electrons and its transit-time damping are drastically reduced. The enhancement in ξ^2 reaches a maximum (a factor of 5) at this magnetic field. This experiment was also performed in an afterglow plasma in which the primary electrons are no longer present. The initial ξ^2 is higher than with the caviton obtained during the discharge. However, there is

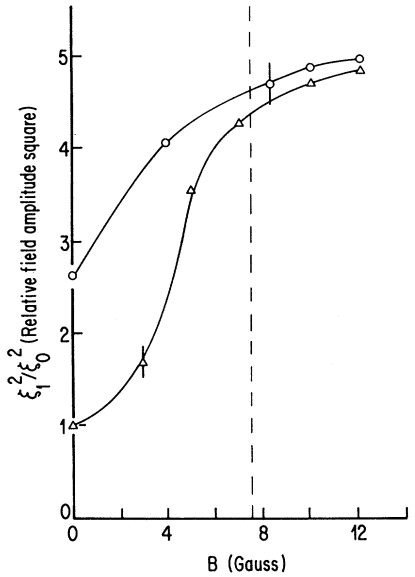

FIG. 2. The enhancement of the electric field in the presence of a weak magnetic field. Δ, steady-state plasma measurement; ○, afterglow plasma measurement. ξ_0 is the field intensity without the magnetic field. The dashed line indicates the theoretical value of the magnetic field at which the transit-time damping by fast electrons is eliminated.

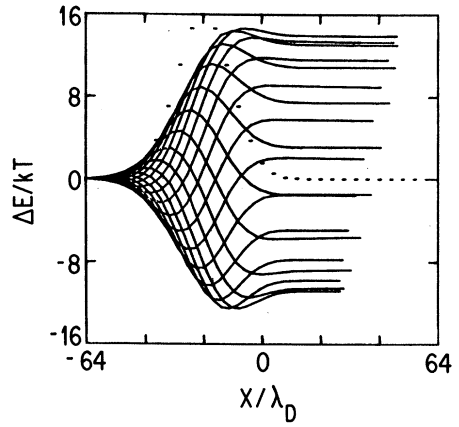

FIG. 3. ΔE vs X diagram to illustrate energy exchange between particles and cavitons for twenty different phases evenly distributed between zero and 2π, for $v_b/v_{th} = 6$ and $\xi^2/4\pi n_0 T = 1$. The positive maximum energy gain is always larger than the maximum negative energy gain for every initial velocity. The dashed line indicates the localized E field profile.

only a mild enhancement by the magnetic field because the population of fast electrons is small to start with. We wish to point out that this result is relevant in understanding the physics behind caviton formation in the ionosphere ($\omega_c/\omega_p \approx 0.2$) and laser-plasma interactions in the presence of self-generated magnetic fields ($\omega_c/\omega_p \approx 0.04$).[9]

When electrons pass through the caviton they gain or lose energy depending on their phase with respect to the coherent oscillations of the caviton field. An electron distribution with a finite spread always gains energy according to a second-order calculation in which the orbit perturbation is taken into account.[2] Consider a particle entering the caviton region at a particular phase of the rf field (Fig. 3). If the phase is favorable, the particle is accelerated to a higher velocity and continues to gain energy. However, if the same particle is initially decelerated to a lower velocity and spends more time inside the caviton, thereby sampling electric fields of alternate signs, it will not gain as much energy from the caviton as it would at the optimum phase. After averaging over all the possible phases at which a distribution of particles can interact with a caviton, there is found a net drain of energy from the caviton.

The phase-coherent feature of particle-caviton interaction is only evident if the particle distribution is modulated both in velocity and in time, i.e., bursts of particles are constrained to encounter the caviton at a particular phase of its oscillation cycle. In another experiment we have deliberately superimposed a sinusoidal modulation on our injected electron beam flux through the acceleration grid. As can be observed in Fig. 4, only at a certain phase angle is there a significant reduction in the caviton field. Although the-

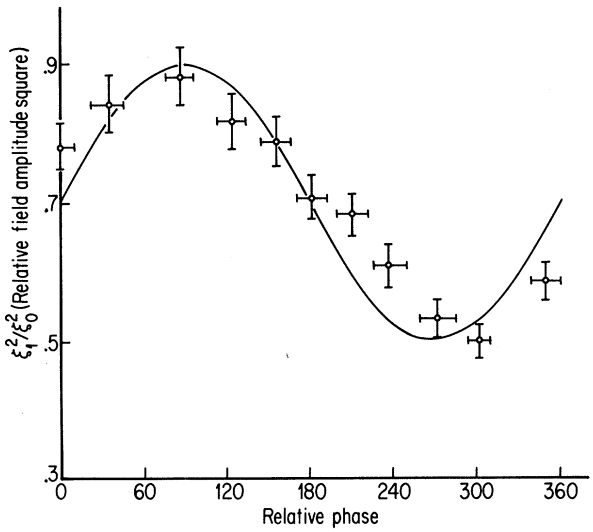

FIG. 4. The relative field intensity as a function of the relative phase between the beam and resonant field. $\bar{v}_b/v_{th} = 4$, $n_b/n_0 = 1\%$, $\xi_0^2/4\pi n_0 T \approx 1$.

oretically cavitons can gain energy from bursts of beam electrons, no net enhancement has yet been observed in the experiment because all the beam electrons would have to undergo very sharp modulation in density and velocity in order to avoid transit-time damping incurred by any slight velocity spread or out-of-phase particles. Our calculations indicate that the phase angle must be controlled to within $\Delta\theta \leq \pi$. Thus $(\Delta v/v)/(x_0/v)\omega < \pi$, where x_0 is the distance from the modulation grid to the caviton. For our experimental conditions this requires an energy spread of 0.1 eV as compared with our present value of 5 eV.

To explain our experimental results quantitatively we consider the energy transport from the caviton region according to the following equation:

$$v_g \xi^2/4\pi + \langle \int_{-\infty}^{\infty} vf(v)E(v)dv \rangle_{av} = p_{ext}, \quad (1)$$

where the average is taken over all possible phases in the particle-caviton interaction and E is the energy exchange. The first term describes wave convection; the second, transit-time damping; and the right-hand side, the pump. All quantities on the left-hand side are evaluated at the boundaries of the caviton.

By following particle trajectories through a caviton by computer we found that the transit-time damping is essentially given within our parameter range by

$$\int_{-\infty}^{\infty} vf(v)Edv = nV(\bar{v})\xi^2/4\pi n_0 .$$

The energy exchange E is the maximum ponderomotive potential energy $\xi^2/4\pi n_0$ modified by an effective group velocity V which is a function of the mean velocity of the distribution $\bar{v}$.

The equations governing our injected-electron-beam experiment can be obtained by using this result in Eq. (1). For the same pump strength, we get one equation for the case with an injected beam (peak electric field = ξ_1) and one equation for the case without (peak electric field = ξ_0). Combining these two equations gives

$$\frac{\xi_1^2}{\xi_0^2} = \frac{v_g + (n/n_0)V(v_{th})}{v_g + (n/n_0)V(v_{th}) + (n_b/n_0)V(v_b)}, \quad (2)$$

where n_0 and v_{th} are the background density and mean velocity, respectively, and n_b and v_b are the beam density and mean velocity, respectively. This result is found to yield good agreement between theory and experiment in Fig. 1.

In order to explain the phase dependence in Fig. 4 we denote the phase-sensitive portion of the beam by $\delta n_b \cos\theta$. Equation (2) then becomes

$$\xi_1^2/\xi_0^2 \approx A[1 - (\delta n_b/n_0)\cos\theta]$$

for $\delta n_b \ll n_b$, where A is constant. This is in agreement with the experimental data in Fig. 4.

In a collisionless plasma where particles retain their phase information, cavitons can be regenerated in the following manner: Consider a density gradient subject to the excitation of two or more frequencies ω_1, ω_2. Two cavitons are established at their resonant locations separated by a distance L. Particles passing through these cavitons are bunched into beams at favorable phases and are effectively modulated at all harmonics of the caviton frequency. The velocity distribution undergoes a perturbation $\sum_n f_1(v, n\omega) \times \exp[-in\omega t + i(n\omega/v)x]$. By use of a treatment similar to plasma echoes it can be shown[10] that after traversing through two cavitons particles will regroup at echo locations $x = [n\omega_2/(n\omega_2 - m\omega_1)]L$ oscillating at frequencies $\omega = n\omega_2 - m\omega_1$. If such locations and frequencies also satisfy $\omega = \omega_p(x)$ then new cavitons are formed. Thus particles may serve as the intermediary between stationary cavitons, continuously destroying and creating cavitons.

In summary, we have demonstrated the importance of kinetic effects in the physics of cavitons. Only in the presence of a weak magnetic field, where transit-time damping is greatly reduced, can the usual fluid theories be applied.

We wish to acknowledge valuable discussions with Dr. G. Morales. This work was supported by the U. S. Air Force Office of Scientific Research under Grant No. 72-2332.

[1]H. C. Kim, R. L. Stenzel, and A. Y. Wong, Phys. Rev. Lett. 33, 886 (1974).

[2]G. J. Morales and Y. C. Lee, Phys. Rev. Lett. 33, 1534 (1974).

[3]E. J. Valeo and W. L. Kruer, Phys. Rev. Lett. 33, 750 (1974).

[4]A. Ishida and K. Nishikawa, J. Phys. Soc. Jpn. 38, 1553 (1975); B. Bezzerides and D. F. DuBois, Phys. Rev. Lett. 34, 1381 (1975); L. I. Rudakov, Dokl. Acad. Nauk 207, 821 (1972) [Sov. Phys. Dokl. 17, 1166 (1973)]; V. V. Gorev and T. K. Soboleva, Phys. Lett. 53A, 347 (1975).

[5]R. J. Taylor, K. R. MacKenzie, and H. Kiezi, Rev. Sci. Instrum. 45, 1675 (1972).

[6]P. D. Goldan and W. M. Leavens, Phys. Fluids 13, 433 (1970); R. S. Harp, W. B. Cannara, F. W. Crawford, and G. S. Kino, Rev. Sci. Instrum. 36, 960 (1965).

[7]A. Y. Wong, University of California at Los Angeles Report No. PPG-277 (unpublished), and TRW Systems Report No. 26266-6002-RU-00, 1977 (unpublished).

[8]H. Injeyan, P. Leung, and A. Y. Wong, Bull. Am. Phys. Soc. 21, 1093 (1976).
[9]J. A. Stamper and B. H. Ripin, Phys. Rev. Lett. 34, 138 (1975); W. F. DiVergilio, A. Y. Wong, H. C. Kim, and Y. C. Lee, Phys. Rev. Lett. 38, 541 (1977).
[10]R. W. Gould, T. M. O'Neil, and J. H. Malmberg, Phys. Rev. Lett. 19, 219 (1967); D. R. Baker, N. R. Ahern, and A. Y. Wong, Phys. Rev. Lett. 20, 7 (1968).

Extended X-Ray-Absorbtion Fine-Structure Beats: A New Method to Determine Differences in Bond Lengths

G. Martens, P. Rabe, N. Schwentner, and A. Werner
Institut für Experimentalphysik, Universität Kiel, Kiel, Germany
(Received 28 June 1977)

The superposition of two scattering shells produces beats in the envelope function of the extended x-ray–absorption fine-structure spectrum and a modulation in the scattering phases. From the k values of the extrema in the envelope function and from the inflection points of the phases the separation of these shells can be calculated without knowledge of the scattering phases of the single shells. A resolution in R space up to 0.02 Å can be obtained even in cases where methods used so far are not able to resolve the scattering shells.

Absorption spectra of polyatomic systems show a modulation of the absorption coefficient above the ionization energies of inner shells. It has been attributed to an interference of the ejected photoelectrons at the site of the absorbing atom. For K-shell excitation the modulating part of the absorption coefficient called the extended x-ray–absorption fine structure (EXAFS) is described by

$$\chi(k) = -k^{-1}\sum_i A_i(k)\sin[2kR_i + \varphi_i(k)] \qquad (1)$$

with

$$A_i(k) = (N_i/R_i^2)\,|f_i(\pi, k)|\exp(-2\sigma_i^2k^2 - 2R_i/\lambda),$$

where N_i is the number of atoms in the ith shell at a distance R_i to the absorbing atom, $|f_i(\pi, k)|$ is the amplitude for scattering through angle $\theta = \pi$. σ_i^2 describes the mean-square displacement of the atoms from their average positions. The mean free path λ of the electrons takes into account the observed decreasing contribution of more distant shells. The phase shift $\varphi(k)$ is due to the influence of the potentials of the absorbing atom and the scattering atoms on the electron wave.

Several attempts have been made to extract structural information from EXAFS. The most general methods used are fitting procedures[1,2] and Fourier transform methods.[3-6] A fitting procedure is limited to simple fine structures built up from one or two scattering shells because of the rapidly increasing number of parameters for more shells. The Fourier transform method can be applied to more complicated structures. From $\chi(k)$ a radial structure function $|F(r)|$ can be derived. The maxima of this function are generated by shells of scattering atoms surrounding the absorbing atom. The positions of the peaks in $|F(r)|$ are shifted compared to the true distances due to contributions of the scattering phases that depend on k.

Several problems for the determination of atomic distances arise from this Fourier transform method: (i) The scattering phases in general are unknown. Major efforts have been made to calculate the phases[7] or to extract them from experimental data.[6,8] The transferability of phase shifts has been emphasized especially.[8] (ii) The reference energy necessary for the conversion of the energy scale to the k scale is unknown. Usually the inflection point of the K edge is used to fix the k scale. This arbitrary choice leads to distortions, especially in the low-k-value region. (iii) Because the range in k space where EXAFS can be observed with sufficient amplitudes is limited, the radial structure function yields broadened features. The widths of these features determine the resolution in R space especially for close-lying shells.

Here an extended Fourier transform method will be presented for pairs of scattering shells. It will be shown that the resolution in R space can be improved compared to the Fourier transform methods used up to now. Further, in contrast to usual Fourier transformations, a knowledge of the phase is not necessary to determine in bond lengths.

We consider an EXAFS spectrum for two con-